

Tidal variability in the Hong Kong region

Adam T. Devlin

Department of Geography and the Environment, Jiangxi Normal University.

Nanchang, Jiangxi, China

Institute of Space and Earth Information Science, The Chinese University of Hong Kong, Shatin,

Hong Kong SAR, China

Shenzhen Research Institute, The Chinese University of Hong Kong, Shenzhen, Guangdong, China

Jiayi Pan*

Department of Geography and the Environment, Jiangxi Normal University.

Nanchang, Jiangxi, China

Institute of Space and Earth Information Science, The Chinese University of Hong Kong, Shatin,

Hong Kong SAR, China

Shenzhen Research Institute, The Chinese University of Hong Kong, Shenzhen, Guangdong, China

Hui Lin

Department of Geography and the Environment, Jiangxi Normal University.

Nanchang, Jiangxi, China

Institute of Space and Earth Information Science, The Chinese University of Hong Kong, Shatin,

Hong Kong SAR, China

* - Corresponding author

Second re-submission to *Ocean Science*

May 2019

Abstract

32
33
34
35
36
37
38
39
40
41
42
43
44
45
46
47
48
49
50
51
52
53
54
55
56
57
58
59
60

Mean sea level (MSL) is rising worldwide, and correlated changes in ocean tides are also occurring. This combination may influence future extreme sea levels, possibly increasing coastal inundation and nuisance flooding events in sensitive regions. Analyses of a set of tide gauges in Hong Kong reveal complex tidal behavior. Most prominent in the results are strong correlations of MSL variability to tidal variability over the 31-year period of 1986-2016; these tidal anomaly correlations (TACs) express the sensitivity of tidal amplitudes and phases (M_2 , S_2 , K_1 , O_1) to MSL fluctuations and are widely observed across the Hong Kong region. At a few important harbor locations, time series of approximations of the parameter δ -HAT, computed from combinations of the major tidal constituents, are found to be highly sensitive to MSL variability which may further increase local flood levels under future MSL rise. Other open-water locations in Hong Kong only show TACs for some individual tidal constituents but not for combined tidal amplitudes, suggesting that the dynamics in enclosed harbor areas may be partially frequency-dependent and related to resonance or frictional changes. We also observe positive correlations of the fluctuations of diurnal (D_1) tides to semidiurnal (D_2) tides at most locations in the region which may lead to further amplified tidal ranges under MSL. Overall, it is shown that tidal changes in the Hong Kong coastal waters may be important in combination with MSL rise in impacting future total water levels.

61

62 ***1. Introduction***

63 Ocean tides have long been thought of as a stationary process, as they are driven by
64 the gravitational forcing of the Sun and Moon whose motions are complex but highly
65 predictable (Cartwright and Tayler, 1971). Yet, long-term changes in the tides have been
66 observed recently on regional (Ray, 2006; Jay et al., 2009; Zaron and Jay, 2014; Rasheed and
67 Chua, 2014; Feng et al., 2015; Ross et al., 2017) and worldwide spatial scales (Woodworth,
68 2010; Müller, et al. 2011; Haigh et al., 2014; Mawdsley et al., 2015), concurrent with long-
69 term global mean sea level (MSL) rise (Church and White, 2006; 2011). Since gravitational
70 changes are not the reason, the tidal changes are likely related to terrestrial factors such as
71 changes in water depth which can alter friction (Arbic et al, 2009), coastal morphology and
72 resonance changes of harbor regions (Cartwright, 1972; Bowen and Gray, 1972; Amin, 1983;
73 Vellinga et al., 2014; Jay et al., 2011; Chernetsky et al., 2010, Familkhalili & Talke, 2016), or
74 stratification changes induced by increased upper-ocean warming (Domingues et al., 2008;
75 Colosi and Munk, 2006; Müller, 2012; Müller et al., 2012), all of which are also related to
76 sea level rise.

77 Tides can also exhibit short-term variability correlated to short-term fluctuations in
78 MSL (Devlin et al., 2014; 2017a; 2017b). These variabilities may influence extreme water
79 level events, such as storm surge or nuisance flooding (Sweet and Park, 2014; Cherqui et al.,
80 2015; Moftakhari et al., 2015; 2017; Ray and Foster, 2016; Buchanan et al., 2017). Such
81 short-term extreme events are obscured when only considering long-term linear trends. Any
82 significant additional shorter-term positive correlation between tides and sea level
83 fluctuations may amplify this variability and would imply that flood risk based only on the
84 superposition of present-day tides and surge onto a higher baseline sea level will be
85 inaccurate in many situations. The analysis of the correlations between tides and sea level at a
86 local or regional scale can indicate locations where tidal evolution should be considered as a
87 substantial complement to sea level rise. Moreover, since storm surge is a long wave, factors
88 affecting tides can also alter storm surge (Familkhalil and Talke, 2016; Arns et al., 2017).
89 Hong Kong is often subject to typhoons, with some recent storms yielding anomalously high
90 storm surges, so this issue is of critical interest if all such factors are undergoing change.

91 Recent works surveyed tidal anomaly correlations (TACs) at multiple locations in the
92 Pacific, a metric that quantifies the sensitivity of tides to short-term sea level fluctuations

93 (Devlin et al., 2014; Devlin et al., 2017a), finding that over 90% of tide gauges analyzed
94 exhibited some measure of correlation in at least one tidal component. In a related work
95 (Devlin et al., 2017b), the combined TACs of the four largest tidal components was
96 calculated as a proxy for what can be described as changes in the highest astronomical tide
97 (δ -HAT), with 35% of gauges surveyed exhibiting a sensitivity of δ -HATs to sea level
98 fluctuations of at least ± 50 mm under a 1-m sea level change ($\sim 5\%$). A step-by-step
99 description of the TAC and δ -HAT methods, including the details of the calculations of the
100 regressions and statistics can be found in the supplementary materials of Devlin et al. (2017a
101 and 2017b), and in this paper we summarize the meaning and interpretations of the TACs and
102 the δ -HATs in the Appendix.

103 A recent paper performed a similar analysis approach in the Atlantic Ocean, finding
104 comparable results to the Pacific (Devlin et al., 2019). Comparing all worldwide locations
105 found that the greatest (positive) δ -HAT response was seen in Hong Kong (+ 650 mm m⁻¹). A
106 probability distribution function analysis revealed that an extreme sea level exceedance
107 which includes tidal changes can be nearly double (+150 mm) that which only considers
108 MSL exceedance alone (+78 mm) over the past 50 years (Devlin et al., 2017b). However,
109 this approach did not consider water level extremes due to non-tidal or non-MSL factors,
110 such as storm surge, which may further complicate extreme water levels. Yet, even without
111 storm surge included, it was demonstrated that the non-stationarity of tides can be a
112 significant contributor to total (non-storm) water levels in this region and warrants closer
113 examination. Furthermore, tides and storm surge are both long-wave processes and may be
114 sensitive to the same forcing factors, so the behavior of tides may be a possible instructor of
115 the future behavior of storm surge events.

116 Hong Kong and the Pearl River Delta (PRD) region contains many densely-populated
117 areas with extensive coastal infrastructure and significant and continuous recent land
118 reclamation projects. Sea level rise in the region has exhibited a variable rate in the region
119 over the past 50 years (Li and Mok, 2012; Ip and Wai, 1990), but a common feature of all sea
120 level records in the South China Sea (SCS) is a steep increase in the late 1990s with a
121 subsequent decrease in the early 2000s, followed by a sustained increase to the present day.
122 In addition to this variable MSL behavior, there are also anomalous tidal events observed at
123 gauges in semi-enclosed harbor regions during the late 1990s and early 2000s (shown and
124 discussed below), corresponding to times of both rapidly changing sea level and aggressive
125 land reclamation. In this study, we perform a spatial and temporal analysis of tidal

126 sensitivity to MSL variations in Hong Kong using the tidal anomaly correlation (TAC)
127 method at 12 closely-located tide gauges.

128 **2. Methods**

129 *2.1 Data sources*

130 A set of 12 tide gauge records in the Hong Kong region were provided by the Hong
131 Kong Observatory (HKO) and the Hong Kong Marine Department (HKMD), spanning from
132 12 to 63 years in length, including two gauges that are “historical” (i.e., no longer
133 operational). The longest record is the North Point/Quarry Bay tide gauge, located in
134 Victoria Harbor, established originally in 1952 and relocated from North Point to Quarry Bay
135 in 1986. The datums were adjusted and quality controlled by HKO to provide a continuous
136 record (Ip and Wai, 1990). Another long and continuous record is located at Tai Po Kau
137 inside Tolo Harbor. Gauge locations in Hong Kong are shown in Figure 1, with the gauges
138 from HKO indicated by green markers, gauges from HKMD by light blue, and historical
139 (non-operational) gauges by red. Four of six of the HKO gauges (Quarry Bay, Tai Po Kau,
140 Tsim Bei Tsui, and Waglan Island) are sea level pressure transducer types of gauges, and the
141 other two (Shek Pik and Tai Miu Wan) are pneumatic type tide gauges. The Quarry Bay
142 gauge was updated from a float type gauge recently (2017), and the Tai Po Kau gauge was
143 also updated from a float gauge in 2006, and all gauges operated by the HK Marine
144 Department were all set up in 2004 as sea level pressure transducers
145 (<https://www.hko.gov.hk/publica/pubsmo.htm>).

146 Figure 2 shows the geographical setting of the South China Sea, with the location of Hong
147 Kong indicated by the red box. Table 1 lists the metadata for all locations, including station
148 name and station code, latitude and the ranges of the data records used in this study. 2.2

149 *Tidal admittance calculations*

150 Our investigations of tidal behavior use a tidal admittance method. The tidal
151 admittance is the unitless ratio of an observed tidal constituent to the corresponding tidal
152 constituent in the astronomical tide generating force expressed as a potential, V . This
153 potential can then be divided by the acceleration due to gravity, g , to yield $Z_{poi}(t) = V/g$, with
154 units of length that can be compared to tidal elevations, $Z_{obs}(t)$. Yearly harmonic analyses
155 are performed on both $Z_{obs}(t)$ and $Z_{poi}(t)$ at each location, using the R_T_TIDE package for
156 MATLAB (Leffler and Jay, 2009), a robust analysis suite based on T_TIDE (Pawlowicz,

157 2002). The tidal potential is determined based on the methods of Cartwright and Tayler
158 (1971).

159 The result from a single harmonic analysis of $Z_{obs}(t)$ or $Z_{pot}(t)$ determines an amplitude,
160 A , and phase, θ , at the central time of the analysis window for each tidal constituent, with
161 error estimates. A moving analysis window (e.g., at mid-year) produces an annual time-
162 series of amplitude, $A(t)$, and phase, $\theta(t)$, with the complex amplitude, $\mathbf{Z}(t)$, given by:

$$163 \quad \mathbf{Z}(t) = A(t)e^{i\theta(t)} \quad (1)$$

164 The tidal admittance (\mathbf{A}) and phase lag (\mathbf{P}) are formed using Eqs. (2) and (3)

$$165 \quad \mathbf{A}(t) = abs \left| \frac{\mathbf{Z}_{obs}(t)}{\mathbf{Z}_{pot}(t)} \right| , \quad (2)$$

$$166 \quad \mathbf{P}(t) = \theta_{obs}(t) - \theta_{pot}(t) \quad (3)$$

167 Nodal variabilities are typically present with similar strengths in both the observed
168 tidal record and in the tidal potential. Therefore, when the observed data (harmonically
169 analyzed in one-year windows) is divided by the potential (also analyzed in one-year
170 windows), nodal effects are mostly constrained in the resulting admittance time series. This
171 may not always hold true in shallow-water areas (Amin, 1983) but does seem to valid for the
172 locations and tides analyzed in Hong Kong. The harmonic analysis procedure also provides
173 an annual MSL time-series. For each resultant dataset (MSL, \mathbf{A} and \mathbf{P}), the mean and trend
174 are removed from the time series to allow direct comparison of their co-variability. The
175 magnitude of the long-term trends is typically much less than the magnitude of the short-term
176 variability, which more apparent in the data sets used here (Devlin et al., 2017a; 2017b).

177 Tidal sensitivity to sea level fluctuations is quantified using tidal anomaly correlations
178 (TACs), the relationships of detrended tidal variability to detrended MSL variability (see
179 Appendix). With the use of the TACs we determine the sensitivity of the amplitude and phase
180 of individual constituents (M_2 , S_2 , K_1 , O_1) to sea level perturbations at the yearly-analyzed
181 scale. We also consider a proxy for the change in the approximate highest astronomical tide
182 (δ -HAT; see Appendix for details). The approximate δ -HAT reflects the maximum tide-
183 related water level that would be obtained in a year from a combination of time-dependent
184 amplitudes and phases of the four largest tidal amplitudes (M_2 , S_2 , K_1 , and O_1) extracted by
185 the admittance method, typically $\sim 75\%$ of the full tidal range..

186 The detrended time series of the year-to-year change of the δ -HATs are compared to
187 detrended yearly MSL variability in an identical manner as the TACs, and both are expressed
188 in units of millimeter change in tidal amplitude per 1-meter fluctuation in sea level (mm m^{-1}).
189 These units are adopted for convenience, though in practice, the observed fluctuations in
190 MSL are on the order of ~ 0.25 m. The phase TACs are reported in units of degree change
191 per 1-meter fluctuation in sea level. The TAC methodology can also be used to examine
192 correlations between different parts of the tidal spectrum. We additionally examine the
193 sensitivity of combined diurnal (D_1 ; $K_1 + O_1$) tidal amplitudes to semidiurnal (D_2 ; $M_2 + S_2$)
194 tidal amplitudes (D_1/D_2 TACs). The units of the D_1/D_2 TACs are dimensionless (i.e.,
195 mm/mm), and statistics are calculated as above.

196 The use of a window of a year in a harmonic analysis may have an influence on the
197 value of the TAC or δ -HAT, e.g. calendar year (Jan-Dec) vs. water year (Oct-Sep). To
198 provide a better estimate of the overall correlations for all data we take a set of
199 determinations of the correlations using twelve distinct year definitions (i.e., one-year
200 windows running from Jan-Dec, Feb-Jan, ..., Dec-Jan.). We take the average of the set of
201 significant determinations (i.e., p -values of < 0.05) as the magnitude of the TAC or δ -HAT.
202 For an estimate of the confidence interval of the TAC or δ -HAT, the interquartile range
203 (middle 50% of the set) is used.

204 For the very long record stations (e.g., Quarry Bay and Tai Po Kau), we only consider
205 the past 31 years for TAC and δ -HAT determinations (Table 1). The TAC values may change
206 over time, so we adopt a common epoch to better match the rest of the Hong Kong tide gauge
207 networks, which are typically ~ 12 -31 years long. Finally, we highlight some anomalous tidal
208 events observed at certain Hong Kong gauges, and discuss the temporal evolution of the tidal
209 characteristics in Hong Kong.

210 **3. Results**

211 The individual TACs for amplitude and phase in Hong Kong are discussed first,
212 followed by the δ -HATs and the D_1/D_2 TACs. In all figures, significant positive results will
213 be reported by red markers, significant negative results by blue markers, and insignificant
214 values are shown as black markers. The relative size of the markers will indicate the relative
215 magnitude of the TAC or δ -HAT according the legend scale on each plot. All numerical
216 results for the major amplitude TACs (M_2 , S_2 , K_1 , and O_1) are listed in Table 2, and the δ -

217 HATs and D₁/D₂ TACs are listed in Table 3. Phase TACs of the individual constituents are
218 reported in Table S1 of the supplement.

219 *3.1 Tidal anomaly correlations (TACs)*

220 The strongest positive M₂ TACs are seen at Quarry Bay ($+218 \pm 37 \text{ mm m}^{-1}$), and at
221 Tai Po Kau ($+267 \pm 42 \text{ mm m}^{-1}$), with a smaller positive TAC seen at Shek Pik (Figure 3).
222 In the waters west of Victoria Harbour, all other gauges except Kwai Chung exhibit moderate
223 negative TACs. The semidiurnal phase TACs in Hong Kong (shown in the Supplementary
224 materials, Figure S1) show an earlier M₂ tide under higher MSL at Quarry Bay and Tai Po
225 Kau and a later tide west of Victoria Harbour. The S₂ results in Hong Kong (Figure 4) show
226 that only Quarry Bay and Tai Po Kau have significant amplitude TAC values (though smaller
227 than M₂), and the S₂ phase TACs in Hong Kong (Figure S2) also show an earlier tide at
228 Quarry Bay and Tai Po Kau under higher MSL.

229 The diurnal TACs in Hong Kong generally exhibit a larger-magnitude and more
230 spatially-coherent response than semidiurnal TACs. Like M₂, the strongest K₁ values in Hong
231 Kong (Fig 5) are seen at Quarry Bay ($+220 \pm 15 \text{ mm m}^{-1}$) and Tai Po Kau ($+190 \pm 68 \text{ mm m}^{-1}$).
232 The O₁ results in Hong Kong (Fig 6) are like the M₂ results, showing positive TACs at
233 Quarry Bay ($+146 \pm 11 \text{ mm m}^{-1}$) and Tai Po Kau ($+100 \pm 25 \text{ mm m}^{-1}$), and strongly negative
234 TACs west of Quarry Bay. However, unlike the semidiurnal constituents, the phase TACs
235 for K₁ are mostly insignificant in Hong Kong (Figure S3), and O₁ phase TACs (Figure S4)
236 are only significant at Quarry Bay.

237 *3.2 Combined tidal variability (δ -HATs) and tidal co-variability*

238 The TACs are widely observed in Hong Kong, but the δ -HATs are only of
239 significance at particular locations (Figure 7). Five stations exhibit significant δ -HAT values,
240 with Quarry Bay and Tai Po Kau having very large positive magnitudes ($+665 \pm 85 \text{ mm m}^{-1}$
241 and $+612 \pm 210 \text{ mm m}^{-1}$, respectively), and Shek Pik having a lesser magnitude of $+138 \pm 47$
242 mm m^{-1} . Conversely, Ma Wan and Chi Ma Wan exhibit moderate negative δ -HAT values, (\sim
243 -100 mm m^{-1}). The remainder of gauges (which are mainly open-water locations) have
244 statistically insignificant results for the combined tidal amplitudes, even where some large
245 individual TACs were observed. This shows that the combined tidal amplitude effect as
246 expressed by the δ -HATs is most important in semi-enclosed harbors. The D₁/D₂ TACs are
247 also important in Hong Kong and are seen at almost every location. All significant D₁/D₂
248 TACs results are positive (Figure 8), and at most locations the correspondence is nearly 1-to-

249 1, indicating that a change in D_1 can yield a nearly-identical magnitude change in D_2 , and
250 vice-versa. Smaller magnitude relations are seen in the western areas of the Hong Kong
251 region.

252 *3.3 Anomalous tidal events at Hong Kong harbor locations*

253 The overall temporal behavior of the tidal spectrum at enclosed harbor locations in
254 Hong Kong (Quarry Bay and Tai Po Kau) is especially interesting. In Figure 9, the time
255 series of water level spectrum components are shown for Quarry Bay and Tai Po Kau,
256 presenting the D_1 ($K_1 + O_1$) band (a), the D_2 ($M_2 + S_2$) band (b), and mean sea level (MSL)
257 (c), given as normalized amplitudes with mean values shown in the legends. The magnitude
258 of MSL is given in relation to the Hong Kong Chart Datum as defined by the Hong Kong
259 Observatory. The Chart Datum is defined as 0.146 m below the Hong Kong Principal Datum
260 (HKPD). The HKPD determined for the years 1965-1983 was approximately 1.23 m below
261 MSL. The HKPD has been recently re-determined using data from 1997-2015 to be 1.30 m
262 below MSL. Therefore, all MSL values reported here are given relative to the HKPD for the
263 epoch 1965-1985. (www.hko.gov.hk).

264 Some very notable features of the tides are clear. At Quarry Bay, the early part of the
265 record shows nearly constant tidal amplitudes in D_1 , while D_2 amplitudes show a slight
266 decrease, and MSL exhibits a slight positive trend. In the late 1980s, however, both D_1 and
267 D_2 increase until around the year 2003, at which time both tidal bands undergo a rapid
268 decrease of amplitude of $\sim 15\%$, sustaining this diminished magnitude for about five years
269 before increasing nearly as rapidly. The OT band shows a sustained increase over the
270 historical record, but many of the fluctuations around the trend are negatively correlated with
271 the perturbations in D_1 and D_2 , and during the times of diminished major tides, the OTs
272 increase by about $+20\%$. The MSL record is also highly variable at Quarry Bay, with a
273 nearly zero trend during the increase in tides seen in the 1980s, followed by a strong increase
274 from ~ 1993 -2000, and then a steep decrease concurrent with the time of diminished tides
275 before increasing again. The gauge at Tai Po Kau shows a similar tidal behavior, although
276 the timing and magnitudes are different. The increase in D_1 and D_2 at Tai Po Kau in the
277 1980s is much larger and peaks earlier than Quarry Bay, reaching a maximum around 1996,
278 and then decreasing around 1998, about five years before the drop at Quarry Bay. Both
279 locations experience an absolute minimum around 2007 in D_2 , but the D_1 minimum at TPK

280 leads the Quarry Bay minimum by a few years. These observed anomalies are only observed
281 at these two gauges; other locations in Hong Kong did not reveal similar behavior.

282 **4. Discussion**

283 *4.1 Summary of observed tidal variability*

284 This survey has identified several types of tidal variability in Hong Kong. The
285 individual TACs are significant at many Hong Kong locations, while the TACs of the
286 approximate δ -HATs appear to be more locally important, as the strongest responses are
287 mainly concentrated at specific locations (e.g., Quarry Bay and Tai Po Kau). The M_2
288 response (Fig 3) is negative at gauges just west of Quarry Bay and positive at Shek Pik, with
289 a similar pattern seen for the O_1 TACs (Fig 6). Conversely, the K_1 TAC results are generally
290 positive (Fig 5). At both Quarry Bay and Tai Po Kau, the positive reinforcements of
291 individual tidal fluctuations lead to very large δ -HATs, though moderately negative δ -HATs
292 are seen near Quarry Bay at Chi Ma Wan and Ma Wan (Fig 7). The spatial similarity in the
293 semi-enclosed center harbor regions suggest a connected mechanism; this area is where most
294 recent Hong Kong coastal reclamation projects have occurred, including the construction of a
295 new island for an airport, shipping channel deepening and other coastal morphology changes.
296 Such changes in water depth and coastal geometry strongly suggest a relation to frictional or
297 resonance mechanisms.

298 The D_1/D_2 TAC relations (Fig 8) are a more regionally-relevant phenomenon, being
299 significant nearly everywhere in Hong Kong. The majority of significant D_1/D_2 TACs are
300 positive, with most being nearly 1-to-1 (i.e., a ~ 1 -mm change in D_1 will yield a ~ 1 -mm
301 change in D_2), confirmed by the close similarity of temporal tidal trends of the D_1 and D_2
302 tidal bands in Hong Kong (Fig 9). This aspect of tidal variability in Hong Kong may be
303 related to the dynamics near the Luzon Strait, where large amounts of baroclinic conversion
304 in both D_1 and D_2 tides may tend to couple the variabilities (Jan et al., 2007; 2008; Lien et al.,
305 2015; Xie et al., 2008; 2011; 2013). The D_1 and D_2 internal tides may interact with each
306 other as well as with processes at other frequencies, such as at the local inertial frequency, f ,
307 via parametric subharmonic instability (PSI) interactions (McComas and Bretherton, 1977;
308 MacKinnon and Winters, 2005; Alford, 2008; Chinn et al., 2012), a form of resonant triad
309 interactions (Craik, 1985). The low-mode baroclinic energy can travel great distances, being
310 enhanced upon arrival at the shelf and leading to the further generation of baroclinic energy.
311 In the western part of Hong Kong, the D_1/D_2 relationships are less than 1 to 1 (~ 0.33 to ~ 0.25

312 at TBT and LOP, respectively). This may be partially influenced by effects of the Pearl River,
313 which discharges part of its flow along the Lantau Channel. The flow of the river is highly
314 seasonal and ejects a freshwater plume at every ebb tide that varies with prevailing wind
315 conditions and with the spring-neap cycle (Pan et al, 2014). The plumes may affect
316 turbulence and mixing in the region and can dissipate tidal energy , which may “decouple”
317 the correlated response of D_1 and D_2 seen in the rest of the Hong Kong coastal waters.

318 *4.2 Effects of local dynamics on tidal variability*

319 Hong Kong has had a long history of land reclamation to accommodate an ever-
320 growing infrastructure and population, including the building of a new airport island (Chep
321 Lap Kok), new land connections, channel deepening to accommodate container terminals,
322 and many bridges, tunnels, and “new cities”, built on reclaimed land. All of these may have
323 changed the resonance and/or frictional properties of the region. Tai Po Kau has also had
324 some land reclamation projects that have changed the coastal morphology and may have
325 modulated the tidal response. Both locations also show coherent D_1/D_2 TACs, as well as
326 having the largest positive δ -HATs, and large tidal anomalies (Figure 9). Other locations in
327 Hong Kong did not show such extreme variations, so these variations appear to only be
328 amplified in harbor areas. Decreases in friction associated with sea level rise may lead to
329 higher forcing of the tides, and those changes may also be amplified by the close correlations
330 of D_1 and D_2 variability or local harbor development which may further decrease local
331 friction. Hence, a small change in friction due to a small sea level change may induce a
332 significant change in tidal amplitudes. The positive reinforcement of multiple tidal
333 constituent correlated with regional sea level adjustments may amplify the risks of coastal
334 inundation and coastal flooding, as evidenced by the gauges that had the largest δ -HAT
335 values.

336 *4.3 Limitations of this study and future steps*

337 The analysis of tides in the Hong Kong tide gauge network revealed new dynamics
338 and spatial connections in the area. However, some records are of shorter length and/or have
339 many gaps, making a full analysis of the area problematic. For example, the Tsim Bei Tsui
340 gauge covers a long period, but there are significant gaps in the record, which complicated
341 our analysis. This gauge is located within a harbor region (Deep Bay), bordered to the north
342 by Shenzhen, PRC, which has also grown and developed its coastal infrastructure in past
343 decades, therefore, one might expect similar dynamics as was seen at Quarry Bay and Tai Po

344 Kau. While there were moderately significant D_1/D_2 correlations at Tsim Bei Tsui, no
345 significant TACs or δ -HATs were observed. The large anomalies seen at Quarry Bay and Tai
346 Po Kau around 2000 are suggested by the data at Tsim Bei Tsui, but some data is missing
347 around this time, making any conclusions speculative. The Deep Bay region is ecologically
348 sensitive, being populated by extensive mangrove forests which may be disturbed by rapidly
349 changing sea levels (Zhang et al., 2018), so accurate determination of future sea levels is of
350 utmost importance to the vitality of these important ecosystems. Future studies considering
351 highly-accurate digital elevation models will employ simple analytical models as well as high
352 resolution three-dimensional numerical ocean models to simulate the changing impacts on
353 coastlines under a variety of sea level, tidal forcing, and anthropogenic change scenarios
354 (historical and future), to better understand the tidal dynamics in Hong Kong, and to try to
355 separate the relative importance of local and regional effects. Lastly, we quickly mention the
356 instrumental changes at two of the HKO gauges. The Quarry Bay gauge was updated from a
357 float type gauge recently (2017), and the Tai Po Kau gauge was also updated from a float
358 gauge in 2006. Neither of these times correspond to any obvious anomalies in the tidal
359 admittance records (the large changes at Tai Po Kau predate this by a few years at least, and
360 are consistent before and after the gauge change), so we conclude that the instrumental
361 changes were not a factor in the observed variability.

362 *5. Conclusions*

363 This study has presented new information about the tidal variability in Hong Kong,
364 based on observations of a set of closely-located tide gauges in Hong Kong. The TACs,
365 D_1/D_2 relations, δ -HATs, and the anomalous events in tidal amplitudes seen at the Quarry
366 Bay and Tai Po Kau gauges show an amplified tidal response to MSL fluctuations in these
367 harbor regions as opposed to more open-water locations, where individual TAC were
368 sometimes significant, but not as much for the δ -HATs. The reason for the observed behavior
369 may be due to changing friction or resonance induced by coastal engineering projects that are
370 only significant at highly local (i.e., individual harbor) scales. Alternatively, the observed
371 behavior could be related to regional South China Sea changes due to climate change (such as
372 increased upper-ocean warming and/or regional stratification and internal tide generation)
373 may also be a factor. It is difficult to separate the local engineering changes from regional
374 climatic changes without closer investigations. However, even without exact knowledge of
375 the relevant mechanisms, these anomalies do suggest that a pronounced change in tidal
376 properties occurred around the year 2000 in Hong Kong, with the effect being most

377 pronounced at gauges in semi-enclosed harbors. Overall, the tidal variability in Hong Kong
378 documented here may have significant impacts on the future of extreme sea level in the
379 region, especially if the strong positive reinforcements hold or increase in coming decades.
380 Short-term inundation events, such as nuisance flooding, may be amplified under scenarios of
381 higher sea levels that lead to corresponding changes in the tides, which may amplify small
382 changes in water levels and/or reductions in friction due to harbor improvements. The δ -
383 HATs and D_1/D_2 TACs results illustrate that the tidal variability of multiple constituents may
384 be additive, and may reinforce MSL changes at some locations, which may further aggravate
385 coastal flooding under MSL future rise. Since tides and storm surge are both long-wave
386 processes, the locations of strong tidal response may also experience an exaggerated storm
387 surge in the near future.

388

389 **Code availability** All code employed in this study was developed using MATLAB, version
390 R2011B. All code and methods can be provided upon request.

391 **Data Availability** The data used in this study from the Hong Kong Observatory (HKO;
392 <http://www.hko.gov.hk>) and the Hong Kong Marine Department (HKMD;
393 <http://www.mardep.gov.hk/en/home.html>) was provided upon request, discussion of
394 intentions of use, and permission from the appropriate agency supervisors. Data used from
395 the University of Hawaii Sea Level Center (UHSLC; <http://www.uhslc.soest.hawaii.edu>) is
396 publicly available.

397

398 **Appendix**

399 **A1. Tidal Anomaly Correlations (TACs)**

400 Tidal admittances are constructed as described above, employing the use of the tidal
401 potential and Eqs. (2) and (3) to constrain the nodal variation present in the observed tidal
402 amplitudes and phases. Our primary interest in this paper is the interannual to decadal
403 variations and not the long-term trends in mean values. Therefore, we first remove the long-
404 term trends and mean values using the MATLAB “detrend” function. The detrended time-
405 series of residual variations in **A** and **P**, and the residual variations in MSL, can now be
406 examined for coherence, using scatter plots, cross-correlations, and regression statistics. We
407 define the tidal anomaly correlation (TAC) as the slope between detrended tidal properties

408 (amplitude and phase) and detrended MSL, expressed as the millimeter change in tidal
409 amplitude per meter of sea level rise (mm m^{-1}). The same approach is used with the phase
410 difference time-series to provide phase anomaly trends, with the trends expressed as degree
411 change in tidal phase per meter of sea level rise (deg m^{-1}). The errors of the TAC
412 determinations are defined as the 95% confidence interval (CI) of the linear trend
413 determination. Trends are deemed significant if the signal-to-noise ratio (SNR) of the linear
414 trend to the associated error is greater than 2.0.

415 **A2. Approximate change in the highest astronomical tide (δ -HAT)**

416 We also construct a “proxy” quantity as an approximate change in the highest
417 astronomical tide (δ -HAT) using an extension of the TAC method. To do this, we combine
418 the tidal admittance amplitudes of the (typically) four largest astronomical tides (M_2 , S_2 , K_1 ,
419 and O_1), then detrend the resultant combined time series as above. Next, we perform a
420 similar scatterplot and regression approach against the detrended MSL time series as was
421 done with the TACs. The benefit of this approach is to give a clear picture of the overall
422 changes in tides related to sea level changes. Some locations may show that the variability in
423 multiple tidal constituents partially “cancel” each other (e.g., semidiurnal tides may have a
424 large positive tendency compared to MSL variability while diurnal tides may have a large
425 negative tendency, resulting in an offsetting of variabilities under MSL changes, and a
426 smaller overall magnitude δ -HAT), while other locations may show a “reinforced” variability
427 (e.g., both diurnal and semidiurnal tides have positive tendencies compared to MSL changes,
428 resulting in an amplified δ -HAT). Thus, the accurate interpretation of the δ -HAT is that it
429 reflects the maximum tide-related water level that would be obtained in a given analysis
430 period (here, one year) from a chosen set of time-dependent amplitudes extracted from the
431 admittance method.

432 Two details about the δ -HAT parameter should be noted here. First, only the
433 amplitude of the tidal admittance can be combined in this manner, as combining the phase
434 variability of multiple frequencies may be inaccurate at worst, and at best is not very helpful.
435 Second, we acknowledge that the use of the term “ δ -HAT” may be somewhat confusing, as
436 previous literature about tidal analysis uses the term “Highest Astronomical Tide” (HAT) to
437 denote the highest water level that can be expected to occur under average meteorological
438 conditions due purely to astronomical forcing in a given epoch. This typical period is 19
439 years, which considers the full nodal cycle. This definition of HAT does not reflect the

440 highest *possible* water level at a given location, since storm surge or other “non-average”
441 meteorological conditions may amplify water levels far above this level on a shorter time
442 scale than a 19-year determination can reveal. The intention behind our chosen nomenclature
443 of the “approximate change in the highest astronomical tide” (δ -HAT) attempts to expand on
444 this concept by considering the “full” tidal variability (not strictly true since the 4 largest
445 tides are only about 75% of the full tidal range, but these tidal components are nearly always
446 stable in one year analyses, so it is a dependable and easily comparable metric) at timescales
447 shorter than a nodal period (~19 years), but longer than a storm surge (~2-5 days) or other
448 meteorological anomalies. Furthermore, our interest is the changes in tidal components that
449 is not due to astronomy or to meteorology. Rather, we show possible changes to tide-related
450 water level modifications due to MSL modifications, which may be important on seasonal to
451 decadal time scales, induced by mechanisms associated with global climate change (e.g.,
452 steric sea level rise due to ice melt, thermal sea level rise due to upper-ocean warming), or to
453 more local effects (such as rapid harbor modifications or land reclamation that adjusts tidal
454 resonance at a particular location).

455 The changes shown by the δ -HATs are important to consider, since a full
456 understanding of the changes in all components and timescales of the tides may better instruct
457 future coastal planning and engineering. The δ -HAT method used here can give important
458 information about possible future water level inundation in coastal locations that are not
459 storm-related, such as nuisance flooding (or, sometimes called “sunny day flooding”). These
460 may be obscured by longer-term analyses of the classical HAT (i.e., 19 years) if changes are
461 more rapid (i.e., year-to-year or season-to-season). However, it should also be reiterated that
462 a good understanding of changes in tides due to changing background water levels may also
463 be instructive about future storm surge related inundation at a location; both tides and storms
464 are long wave processes, so changes in one aspect of water level variability (i.e., a large
465 positive δ -HAT) may also indicate future increase in storm surge levels at the same location.

466

467 **Author Contributions** ATD did all analyses, figures, tables, the majority of writing, and
468 compiled the manuscript. JP provided editing, insight, guidance, and direction to this study.
469 HL provided critical insight and helpful input.

470 **Competing Interests** The authors declare they have no competing interests.

471 **Acknowledgements** This work is supported by The National Basic Research Program of
472 China (2015CB954103), the National Natural Science Foundation of China (project
473 41376035), the General Research Fund of Hong Kong Research Grants Council (RGC)
474 (CUHK 14303818, 402912, and 403113), the Hong Kong Innovation and Technology Fund
475 under the grants (ITS/259/12 and ITS/321/13), and the direct grants of the Chinese University
476 of Hong Kong. The authors also thank the Hong Kong Observatory. In addition to sharing
477 their data archive, they were also a part of the discussions that led to this paper.

478

479

480 **FIGURE CAPTIONS:**

481 **Figure 1** Tide gauge locations in Hong Kong used in this study. Green markers indicate
482 active gauges provided by the Hong Kong Observatory (HKO), light blue markers indicate
483 gauges provided by the Hong Kong Marine Department (HKMD), and red markers indicate
484 historical gauges (once maintained by HKO) that are no longer operational.

485 **Figure 2** Location of Hong Kong in the South China Sea, given by the red box, with some
486 major oceanographic features labelled. Depth is given by the color bar, in units of meters.

487 **Figure 3** Tidal anomaly correlations (TACs) of detrended M_2 amplitude to detrended MSL in
488 Hong Kong, with the marker size showing the relative magnitude according to the legend, in
489 units of mm m^{-1} . Red/blue markers indicate positive/negative TACs, and black markers
490 indicate TACs which are not significantly different from zero.

491 **Figure 4** Tidal anomaly correlations (TACs) of detrended S_2 amplitude to detrended MSL in
492 Hong Kong, with the marker size showing the relative magnitude according to the legend, in
493 units of mm m^{-1} . Red/blue markers indicate positive/negative TACs, and black markers
494 indicate TACs which are not significantly different from zero.

495 **Figure 5** Tidal anomaly correlations (TACs) of detrended K_1 amplitude to detrended MSL in Hong Kong, with the
496 marker size showing the relative magnitude according to the legend, in units of mm m^{-1} .
497 Red/blue markers indicate positive/negative TACs, and black markers indicate TACs which
498 are not significantly different from zero. .

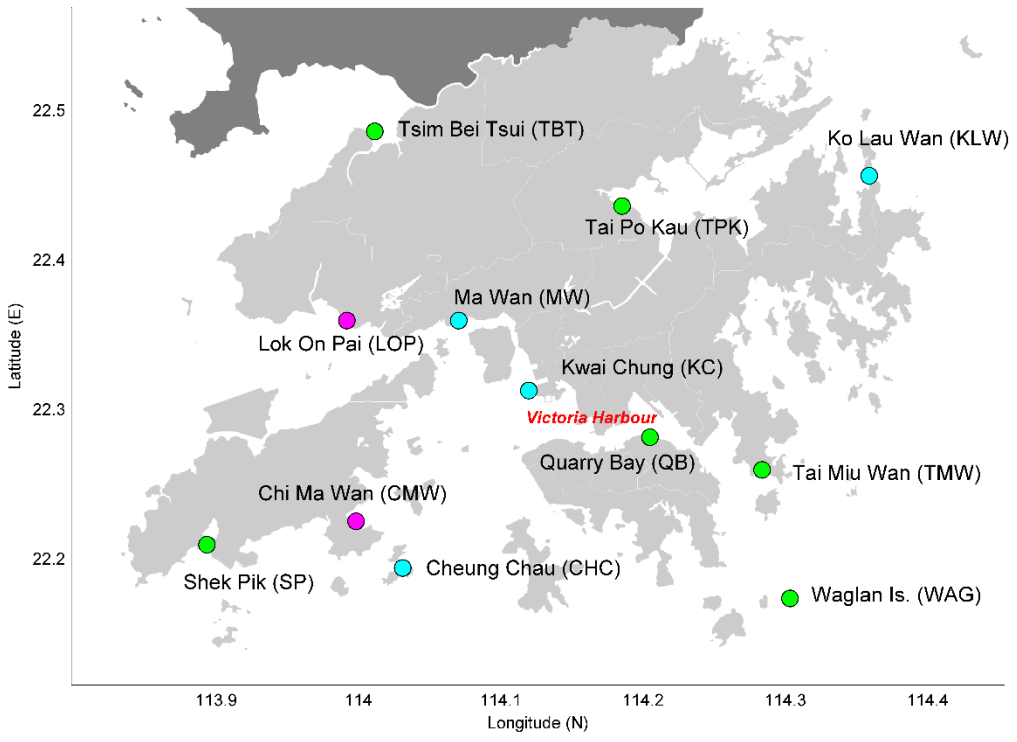
499 **Figure 6** Tidal anomaly correlations (TACs) of detrended O_1 amplitude to detrended MSL in
500 Hong Kong, with the marker size showing the relative magnitude according to the legend, in
501 units of mm m^{-1} . Red/blue markers indicate positive/negative TACs, and black markers
502 indicate TACs which are not significantly different from zero.

503 **Figure 7** The tidal anomaly correlation computed from the combination of the four largest
504 tidal constituent amplitudes (given by the detrended sum of the $M_2 + S_2 + K_1 + O_1$) as a proxy
505 for the change in the approximate highest astronomical tide (δ -HAT) relative to detrended
506 MSL in Hong Kong, with the marker size showing the relative magnitude according to the
507 legend, in units of mm m^{-1} . Red/blue markers indicate positive/negative TACs, and black
508 markers indicate TACs which are not significantly different from zero. **Figure 8** The OT

509 TACs; the relations of detrended diurnal tidal amplitude sum (D_1 ; $K_1 + O_1$) to detrended
 510 semidiurnal tidal amplitude sum (D_2 ; $M_2 + S_2$) in Hong Kong, with the marker size showing
 511 the relative magnitude according to the legend, in dimensionless units. Red/blue markers
 512 indicate positive/negative TACs, and black markers indicate TACs which are not
 513 significantly different from zero. **Figure 9** Time series of water level spectrum components
 514 at the Quarry Bay (QB; blue) and Tai Po Kau (TPK; red) tide gauges in Hong Kong, showing
 515 the D_1 band (a), the D_2 band (b), the OT band (c) and mean sea level (MSL) (d). Components
 516 are plotted as a function of normalized amplitudes to show relative variability, with mean
 517 values given in the legend.

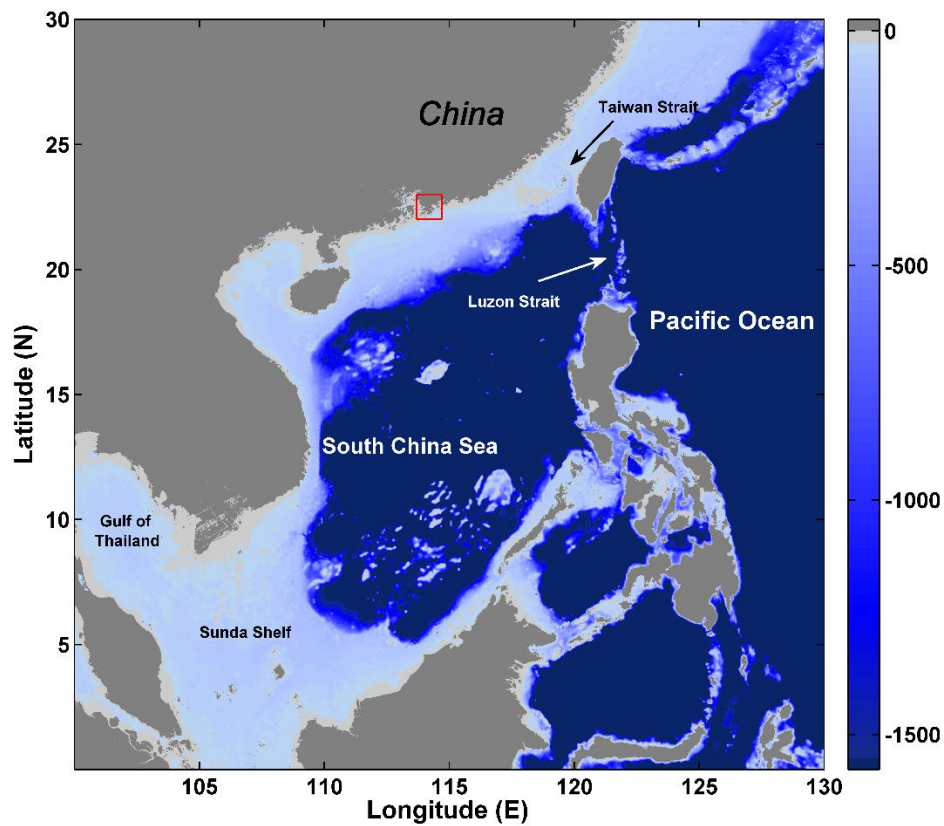
518
 519
 520
 521
 522
 523

524 **FIGURES:**



525
 526 **Figure 1** Tide gauge locations in Hong Kong used in this study. Green markers indicate
 527 active gauges provided by the Hong Kong Observatory (HKO), light blue markers indicate

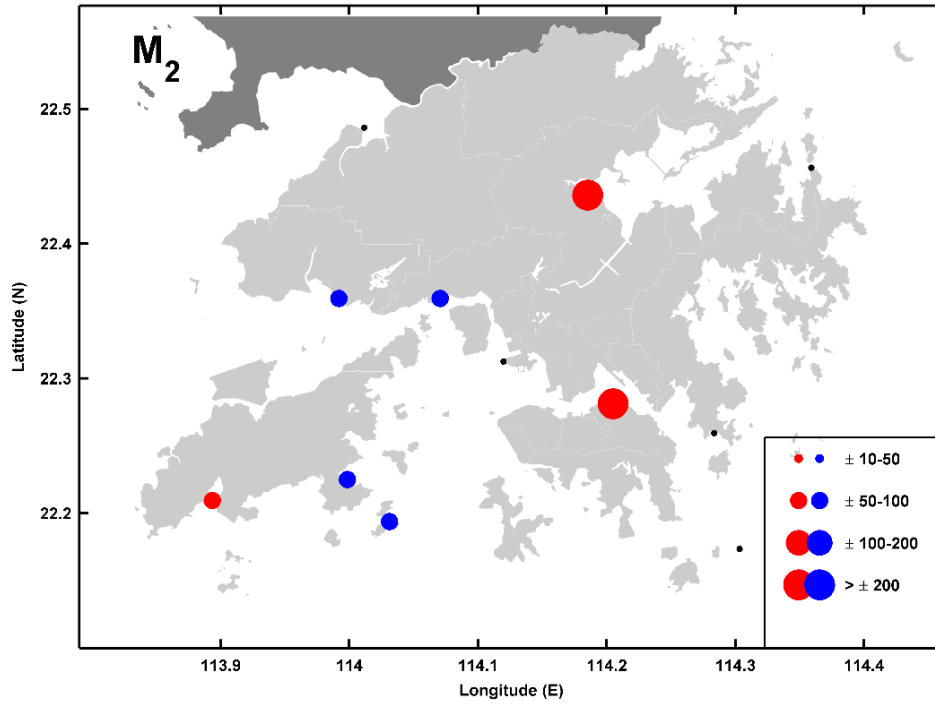
528 gauges provided by the Hong Kong Marine Department (HKMD), and red markers indicate
529 historical gauges (once maintained by HKO) that are no longer operational.



530

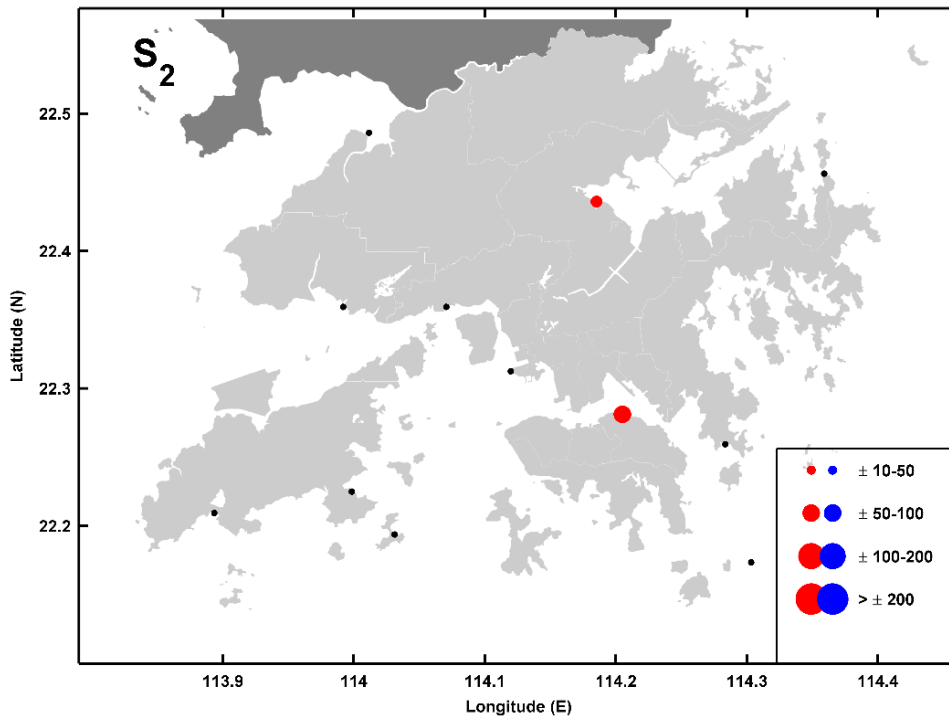
531 **Figure 2** Location of Hong Kong in the South China Sea, given by the red box, with some
532 major oceanographic features labelled. Depth is given by the color bar, in units of meters.

533



534

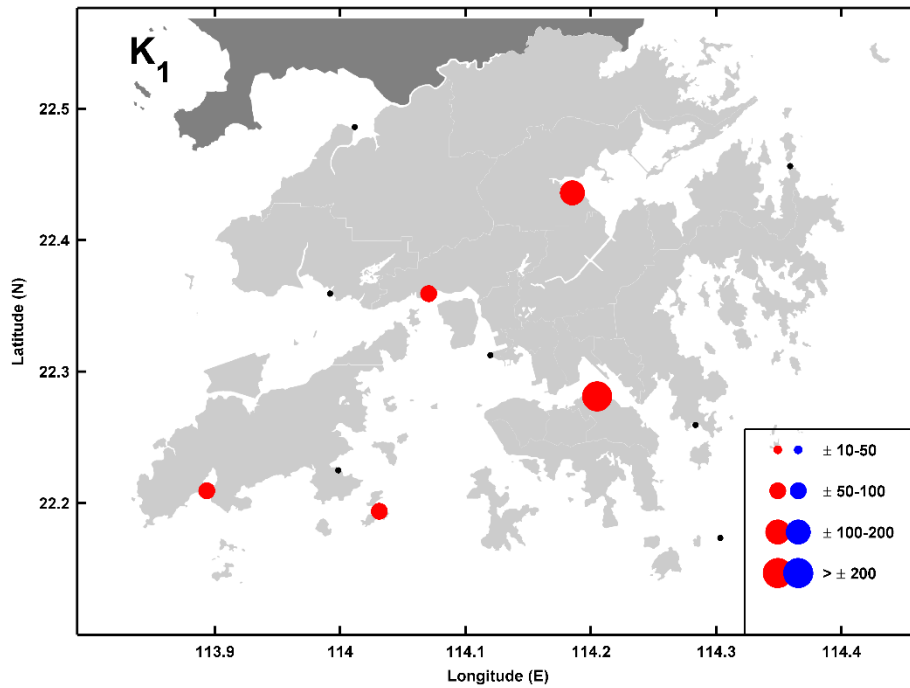
535 **Figure 3** Tidal anomaly correlations (TACs) of detrended M_2 amplitude to detrended MSL in
 536 Hong Kong, with the marker size showing the relative magnitude according to the legend, in
 537 units of mm m^{-1} . Red/blue markers indicate positive/negative TACs, and black markers
 538 indicate TACs which are not significantly different from zero.



539

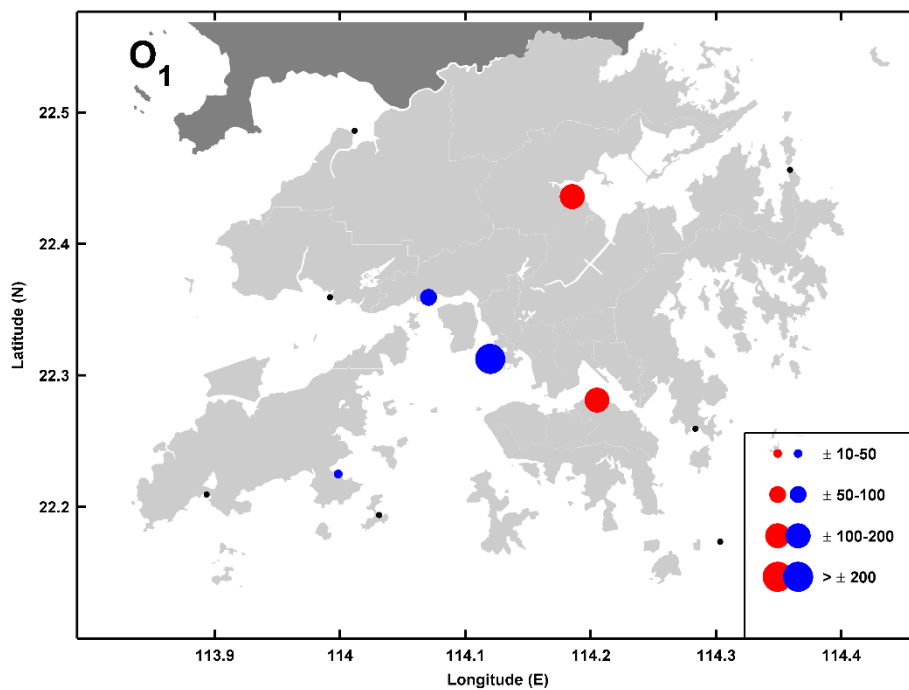
540 **Figure 4** Tidal anomaly correlations (TACs) of detrended S_2 amplitude to detrended MSL in
 541 Hong Kong, with the marker size showing the relative magnitude according to the legend, in
 542 units of mm m^{-1} . Red/blue markers indicate positive/negative TACs, and black markers

543 indicate TACs which are not significantly different from zero.



544

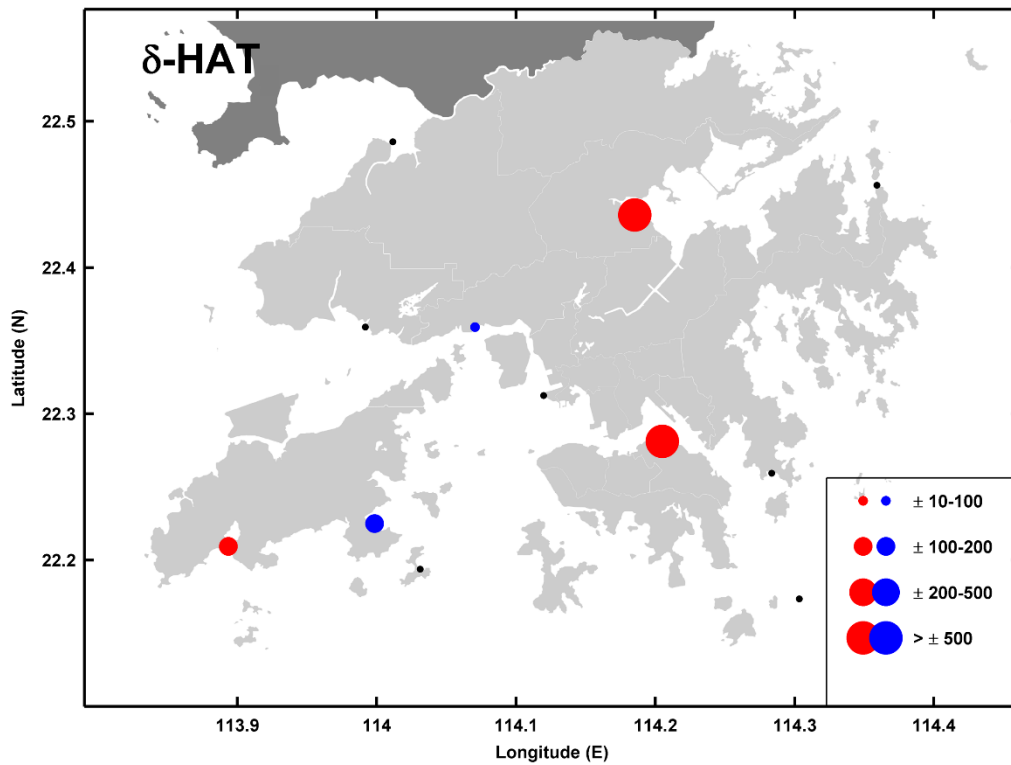
545 **Figure 5** Tidal anomaly correlations (TACs) of detrended K_1 amplitude to detrended MSL in
546 Hong Kong, with the marker size showing the relative magnitude according to the legend, in
547 units of mm m^{-1} . Red/blue markers indicate positive/negative TACs, and black markers
548 indicate TACs which are not significantly different from zero.



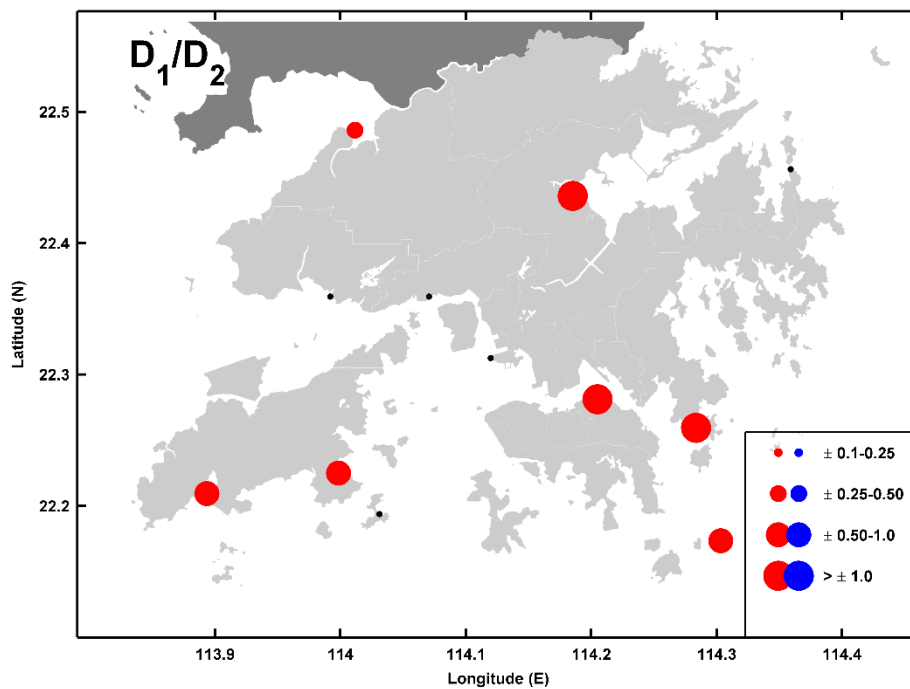
549

550 **Figure 6** Tidal anomaly correlations (TACs) of detrended O_1 amplitude to detrended MSL in
551 Hong Kong, with the marker size showing the relative magnitude according to the legend, in
552 units of mm m^{-1} . Red/blue markers indicate positive/negative TACs, and black markers

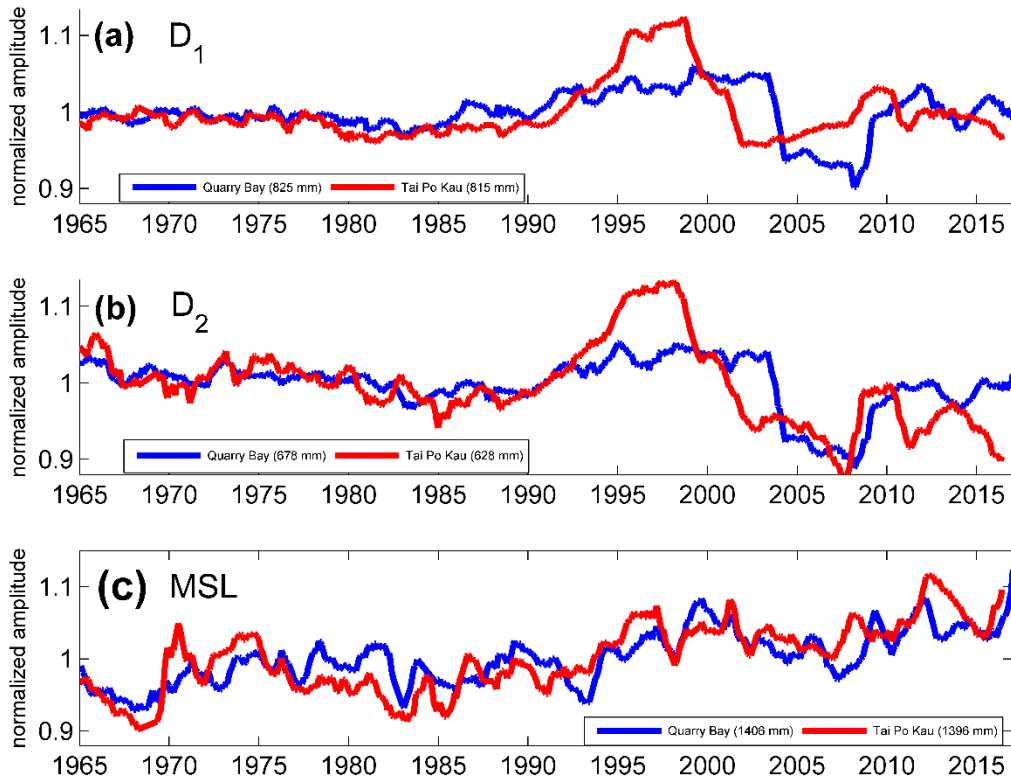
indicate TACs which are not significantly different from zero.



555 **Figure 7** The tidal anomaly correlation computed from the combination of the four largest
 556 tidal constituent amplitudes (given by the detrended sum of the $M_2 + S_2 + K_1 + O_1$) as a proxy
 557 for the change in the approximate highest astronomical tide (δ -HAT) relative to detrended
 558 MSL in Hong Kong, with the marker size showing the relative magnitude according to the
 559 legend, in units of mm m^{-1} . Red/blue markers indicate positive/negative TACs, and black
 560 markers indicate TACs which are not significantly different from zero.



562 **Figure 8** The D_1/D_2 TACs; the relations of detrended diurnal tidal amplitude sum (D_1 ; $K_1 +$
 563 O_1) to detrended semidiurnal tidal amplitude sum (D_2 ; $M_2 + S_2$) in Hong Kong, with the
 564 marker size showing the relative magnitude according to the legend, in dimensionless units.
 565 Red/blue markers indicate positive/negative TACs, and black markers indicate TACs which
 566 are not significantly different from zero.



567
 568 **Figure 9** Time series of water level spectrum components at the Quarry Bay (QB; blue) and
 569 Tai Po Kau (TPK; red) tide gauges in Hong Kong, showing the D_1 band (a), the D_2 band (b),
 570 and mean sea level (MSL) (c). Components are plotted as a function of normalized
 571 amplitudes to show relative variability, with mean values given in the legend.

572
 573
 574
 575
 576
 577
 578
 579
 580

581 **REFERENCES:**

- 582 Alford, M. H.: Observations of parametric subharmonic instability of the diurnal internal tide
583 in the South China Sea. *Geophysical Research Letters*, 35, L15602, 2008.
584 doi:10.1029/2008GL034720
- 585 Amin, M.: On perturbations of harmonic constants in the Thames Estuary. *Geophysical*
586 *Journal of the Royal Astronomical Society*. 73(3): 587-603. doi:10.1111/j.1365-
587 246X.1983.tb03334.x, 1983.
- 588 Arbic, B.K., Karsten, R.H., Garrett, C.: On tidal resonance in the global ocean and the back-
589 effect of coastal tides upon open-ocean tides. *Atmosphere-Ocean* 47(4), 239–266.
590 doi:10.3137/OC311.2009, 2009.
- 591 Arns, A., Dangendorf, S., Jensen, J., Bender, J., Talke, S.A., & Pattiaratchi, C.: Sea level rise
592 induced amplification of coastal protection design heights. *Nature: Scientific Reports*, 7,
593 40171. doi:10.1038/srep40171, 2017.
- 594 Bowen, A. J., & Gray, D. A.: The tidal regime of the River Thames; long-term trends and
595 their possible causes. *Phil. Trans. R. Soc. Lond. A*, 272(1221), 187-199.
596 doi:10.1098/rsta.1972.0045, 1972.
- 597 Buchanan, M. K., Oppenheimer, M., & Kopp, R. E.: Amplification of flood frequencies with
598 local sea level rise and emerging flood regimes. *Environmental Research Letters*, 12(6),
599 064009. doi:10.1088/1748-9326/aa6cb3, 2017.
- 600 Cartwright, D.E., & Tayler, R.J.: New computations of the tide-generating potential. *Geophys.*
601 *Journal of the Royal Astronomical Society*, 23, 45-74. doi: 10.1111/j.1365-
602 246X.1971.tb01803.x, 1971.
- 603 Cartwright, D.E.: Secular changes in the oceanic tides at Brest, 1711–1936. *Geophysical*
604 *Journal International*, 30(4), 433-449. doi:10.1.1.867.2468, 1972.
- 605 Chernetsky, A. S., Schuttelaars, H. M., & Talke, S. A.: The effect of tidal asymmetry and
606 temporal settling lag on sediment trapping in tidal estuaries. *Ocean Dynamics*, 60(5), 1219-
607 1241.. doi: 10.1007/s10236-010-0329-8, 2010.
- 608 Cherqui, F., Belmeziti, A., Granger, D., Sourdril, A., & Le Gauffre, P.: Assessing urban
609 potential flooding risk and identifying effective risk-reduction measures. *Science of the Total*
610 *Environment*, 514, 418-425, 2015.

611 Chinn, B. S., Girton, J. B., & Alford, M. H.: Observations of internal waves and parametric
612 subharmonic instability in the Philippines archipelago. *Journal of Geophysical Research:*
613 *Oceans*, 117(C5). doi:10.1029/2011JC007392, 2012.

614 Church, J. A., & White, N. J.: A 20th century acceleration in global sea-level
615 rise. *Geophysical research letters*, 33(1). doi:10.1029/2005GL024826, 2006.

616 Church, J. A., & White, N. J.: Sea level rise from the late 19th to the early 21st
617 century. *Surveys in geophysics*, 32(4-5), 585-602. doi 10.1007/s10712-011-9119-1, 2011.

618 Colosi, J. A., & Munk, W.: Tales of the venerable Honolulu tide gauge. *Journal of physical*
619 *oceanography*, 36(6), 967-996. doi:10.1175/JPO2876.1, 2006.

620 Craik, A.D.D.: Wave Interactions and Fluid Flows. Cambridge Univ. Press, Cambridge, U. K,
621 ISBN: 978-0521368292, 1985.

622 Devlin, A. T., Jay, D. A., Talke, S. A., & Zaron, E.: Can tidal perturbations associated with
623 sea level variations in the western Pacific Ocean be used to understand future effects of tidal
624 evolution? *Ocean Dynamics*, 64(8), 1093-1120. doi:10.1007/s10236-014-0741-6, 2014.

625 Devlin, A. T., Jay, D. A., Zaron, E. D., Talke, S. A., Pan, J., & Lin, H.: Tidal variability
626 related to sea level variability in the Pacific Ocean. *Journal of Geophysical Research:*
627 *Oceans*, 122(11), 8445-8463. doi:10.1002/2017JC013165, 2017.

628 Devlin, A. T., Jay, D. A., Talke, S. A., Zaron, E. D., Pan, J., & Lin, H.: Coupling of sea level
629 and tidal range changes, with implications for future water levels. *Scientific Reports*, 7(1),
630 17021. doi:10.1038/s41598-017-17056-z, 2017.

631 Devlin, A. T., Zaron, E. D., Jay, D. A., Talke, S. A., & Pan, J.: Seasonality of Tides in
632 Southeast Asian Waters. *Journal of Physical Oceanography*. doi: 10.1175/JPO-D-17-0119.1,
633 2018.

634 Devlin, A. T., Pan, J., & Lin, H.: Extended spectral analysis of tidal variability in the North
635 Atlantic Ocean. *Journal of Geophysical Research: Oceans*, 124(1), 506-526, 2019.

636 Domingues, C. M., Church, J. A., White, N. J., Gleckler, P. J., Wijffels, S. E., Barker, P. M.,
637 & Dunn, J. R.: Improved estimates of upper-ocean warming and multi-decadal sea level
638 rise. *Nature*, 453(7198), 1090. doi:10.1038/nature07080, 2008.

639 Haigh, I. D., Wijeratne, E. M. S., MacPherson, L. R., Pattiaratchi, C. B., Mason, M. S.,
640 Crompton, R. P., & George, S.: Estimating present day extreme water level exceedance

641 probabilities around the coastline of Australia: tides, extra-tropical storm surges and mean sea
642 level. *Climate Dynamics*, 42(1-2), 121-138. doi: 10.1007/s00382-012-1652-1, 2014.

643 Familkhalili, R., & Talke, S. A.: The effect of channel deepening on tides and storm surge: A
644 case study of Wilmington, NC. *Geophysical Research Letters*, 43(17), 9138-9147.
645 doi:10.1002/2016GL069494, 2016.

646 Fang, G., Kwok, Y. K., Yu, K., & Zhu, Y.: Numerical simulation of principal tidal
647 constituents in the South China Sea, Gulf of Tonkin and Gulf of Thailand. *Continental Shelf
648 Research*, 19(7), 845-869. doi: 10.1016/S0278-4343(99)00002-3, 1999.

649 Feng, X., Tsimplis, M. N., & Woodworth, P. L.: Nodal variations and long-term changes in
650 the main tides on the coasts of China. *Journal of Geophysical Research: Oceans*, 120(2),
651 1215-1232. doi:10.1002/2014JC010312, 2015.

652 Ip, S.F. and Wai, H.G.: *An application of harmonic method to tidal analysis and prediction in
653 Hong Kong*. Royal Observatory, 1990.

654 Jan, S., Chern, C. S., Wang, J., & Chao, S. Y.: Generation of diurnal K₁ internal tide in the
655 Luzon Strait and its influence on surface tide in the South China Sea. *Journal of Geophysical
656 Research: Oceans*, 112(C6). doi:10.1029/2006JC004003, 2007.

657 Jan, S., Lien, R. C., & Ting, C. H.: Numerical study of baroclinic tides in Luzon
658 Strait. *Journal of Oceanography*, 64(5), 789. doi:10.1007/s10872-008-0066-5, 2008.

659 Jay, D. A. (2009). Evolution of tidal amplitudes in the eastern Pacific Ocean. *Geophysical
660 Research Letters*, 36(4). doi: 10.1029/2008GL036185

661 Leffler, K. E., & Jay, D. A.: Enhancing tidal harmonic analysis: Robust (hybrid L1/L2)
662 solutions. *Continental Shelf Research*, 29(1), 78-88. doi: 10.1016/j.csr.2008.04.011, 2009.

663 Li, K. W., & Mok, H. Y.: Long term trends of the regional sea level changes in Hong Kong
664 and the adjacent waters. In *Asian And Pacific Coasts 2011* (pp. 349-359).
665 doi:10.1142/9789814366489_0040, 2012.

666 Lien, R. C., Tang, T. Y., Chang, M. H., & d'Asaro, E. A.: Energy of nonlinear internal waves
667 in the South China Sea. *Geophysical Research Letters*, 32(5). doi:10.1029/2004GL022012,
668 2005.

669 MacKinnon, J. A., & Winters, K. B.: Subtropical catastrophe: Significant loss of low-mode
670 tidal energy at 28.9°. *Geophysical Research Letters*, 32(15). doi:10.1029/2005GL023376,
671 2005.

672 Mawdsley, R. J., Haigh, I. D., & Wells, N. C.: Global changes in mean tidal high water, low
673 water and range. *Journal of Coastal Research*, 70(sp1), 343-348. doi:10.2112/SI70-058.1,
674 2014.

675 McComas, C. H., & Bretherton, F. P.: Resonant interaction of oceanic internal
676 waves. *Journal of Geophysical Research*, 82(9), 1397-1412. doi:10.1029/JC082i009p01397,
677 1977.

678 Moftakhari, H. R., AghaKouchak, A., Sanders, B. F., Feldman, D. L., Sweet, W., Matthew,
679 R. A., & Luke, A.: Increased nuisance flooding along the coasts of the United States due to
680 sea level rise: Past and future. *Geophysical Research Letters*, 42(22), 9846-9852.
681 doi:10.1002/2015GL066072, 2015.

682 Moftakhari, H. R., AghaKouchak, A., Sanders, B. F., & Matthew, R. A.: Cumulative hazard:
683 The case of nuisance flooding. *Earth's Future*, 5(2), 214-223. doi:10.1002/2016EF000494,
684 2017.

685 Müller, M., Arbic, B. K., & Mitrovica, J. X.: Secular trends in ocean tides: Observations and
686 model results. *Journal of Geophysical Research: Oceans*, 116(C5) doi:
687 10.1029/2010JC006387, 2011.

688 Müller, M., Cherniawsky, J. Y., Foreman, M. G. G., & Storch, J. S.: Global M₂ internal tide
689 and its seasonal variability from high resolution ocean circulation and tide
690 modeling. *Geophysical Research Letters*, 39(19). doi:10.1029/2012GL053320, 2012.

691 Müller, M.: The influence of changing stratification conditions on barotropic tidal transport
692 and its implications for seasonal and secular changes of tides. *Continental Shelf Research*, 47,
693 107-118. doi: 10.1016/j.csr.2012.07.003, 2012.

694 Pan, J., Gu, Y. and Wang, D.: Observations and numerical modeling of the Pearl River plume
695 in summer season, *Journal of Geophysical Research*, 119, doi:10.1002/2013JC009042, 2014.

696 Pawlowicz, R., Beardsley, B., & Lentz, S.: Classical tidal harmonic analysis including error
697 estimates in MATLAB using T_TIDE. *Computers & Geosciences*, 28(8), 929-937.
698 doi:10.1016/S0098-3004(02)00013-4, 2002.

699 Rasheed, A. S., & Chua, V. P.: Secular trends in tidal parameters along the coast of
700 Japan. *Atmosphere-Ocean*, 52(2), 155-168. doi:10.1080/07055900.2014.886031, 2014.

701 Ray, R. D.: Secular changes of the M₂ tide in the Gulf of Maine. *Continental shelf*
702 *research*, 26(3), 422-427. doi: 10.1016/j.csr.2005.12.005, 2006.

703 Ray, R. D., & Foster, G.: Future nuisance flooding at Boston caused by astronomical tides
704 alone. *Earth's Future*, 4(12), 578-587. doi:10.1002/2016EF000423, 2016.

705 Ross, A. C., Najjar, R. G., Li, M., Lee, S. B., Zhang, F., & Liu, W.: Fingerprints of Sea Level
706 Rise on Changing Tides in the Chesapeake and Delaware Bays. *Journal of Geophysical*
707 *Research: Oceans*, 122(10), 8102-8125. doi:10.1002/2017JC012887, 2017.

708 Sweet, W. V., & Park, J.: From the extreme to the mean: Acceleration and tipping points of
709 coastal inundation from sea level rise. *Earth's Future*, 2(12), 579-600, 2014.

710 Vellinga, N. E., Hoitink, A. J. F., van der Vegt, M., Zhang, W., & Hoekstra, P.: Human
711 impacts on tides overwhelm the effect of sea level rise on extreme water levels in the Rhine–
712 Meuse delta. *Coastal Engineering*, 90, 40-50. doi: 10.1016/j.coastaleng.2014.04.005, 2014.

713 Woodworth, P. L.: A survey of recent changes in the main components of the ocean
714 tide. *Continental Shelf Research*, 30(15), 1680-1691. doi: 10.1016/j.csr.2010.07.002, 2010.

715 Xie, X. H., Chen, G. Y., Shang, X. D., & Fang, W. D.: Evolution of the semidiurnal (M₂)
716 internal tide on the continental slope of the northern South China Sea. *Geophysical Research*
717 *Letters*, 35(13). doi:10.1029/2008GL034179, 2008.

718 Xie, X. H., Shang, X. D., van Haren, H., Chen, G. Y., & Zhang, Y. Z.: Observations of
719 parametric subharmonic instability-induced near-inertial waves equatorward of the critical
720 diurnal latitude. *Geophysical Research Letters*, 38(5). doi:10.1029/2010GL046521, 2011.

721 Xie, X., Shang, X., Haren, H., & Chen, G.: Observations of enhanced nonlinear instability in
722 the surface reflection of internal tides. *Geophysical Research Letters*, 40(8), 1580-1586.
723 doi:10.1002/grl.50322, 2013.

724 Zaron, E. D., & Jay, D. A.: An analysis of secular change in tides at open-ocean sites in the
725 Pacific. *Journal of Physical Oceanography*, 44(7), 1704-1726. doi:10.1175/JPO-D-13-0266.1,
726 2014.

727 Zhang, H., Wang, T., Liu, M., Jia, M., Lin, H., Chu, L. M., & Devlin, A. T.: Potential of
728 Combining Optical and Dual Polarimetric SAR Data for Improving Mangrove Species

729 Discrimination Using Rotation Forest. *Remote Sensing*, 10(3), 467. doi: 10.3390/rs10030467,
730 2018.

731

732

733

734

735

736

737

738

739

740

741

742

743

744

745

746

747

748

749

750

751

752

753

754

755 **TABLES:**

756 **Table 1** Metadata for all tide gauge locations, giving the station names and station codes
757 latitude/longitude, year of the available records, as well as the range of data analyzed.

Station	Latitude	Longitude	Start Year	End Year	Number of years used
Quarry Bay (QB)	22.27° N	114.21° E	1954	2016	31 (1986-2016)

Tai Po Kau (TPK)	22.42° N	114.19° E	1963	2016	31 (1986-2016)
Tsim Bei Tusi (TBT)	22.48° N	114.02° E	1974	2016	31 (1986-2016)
Chi Ma Wan (CMW)	22.22° N	114.00° E	1963	1997	36 (1963-1997)
Cheung Chau (CHC)	22.19° N	114.03° E	2004	2016	12 (2004-2016)
Lok On Pai (LOP)	22.35° N	114.00° E	1981	1999	18 (1981-1999)
Ma Wan (MW)	22.35° N	114.06° E	2004	2016	12 (2004-2016)
Tai Miu Wan (TMW)	22.26° N	114.29° E	1996	2016	20 (1996-2016)
Shek Pik (SP)	22.21° N	113.89° E	1999	2016	17 (1999-2016)
Waglan Island (WAG)	22.17° N	114.30° E	1995	2016	21 (1995-2016)
Ko Lau Wan (KLW)	22.45° N	114.34° E	2004	2016	12 (2004-2016)
Kwai Chung (KC)	22.31° N	114.12° E	2004	2016	12 (2004-2016)

758

759 **Table 2** Amplitude TACs for M_2 , S_2 , K_1 , and O_1 for the period of 1986-2016. All values
760 given are in units of millimeter change in tidal amplitude for a 1-meter fluctuation in sea level
761 (mm m⁻¹). Statistically significant positive values are given in bold italic text.

<i>Station</i>	M_2 TAC	S_2 TAC	K_1 TAC	O_1 TAC
<i>Quarry Bay (QB)</i>	+218 ± 37	+85 ± 16	+220 ± 15	+146 ± 11
<i>Tai Po Kau (TPK)</i>	+267 ± 42	+98 ± 17	+190 ± 68	+100 ± 25
<i>Tsim Bei Tusi (TBT)</i>	+7 ± 80	-10 ± 15	+32 ± 22	+24 ± 22
<i>Chi Ma Wan (CMW)</i>	-58 ± 11	-7 ± 5	-18 ± 8	-37 ± 10
<i>Cheung Chau (CHC)</i>	-63 ± 20	-22 ± 35	+69 ± 48	+50 ± 92
<i>Lok On Pai (LOP)</i>	-81 ± 24	-18 ± 8	+8 ± 32	-24 ± 12
<i>Ma Wan (MW)</i>	-68 ± 4	+1 ± 25	+52 ± 4	-62 ± 21
<i>Tai Miu Wan (TMW)</i>	+22 ± 59	-1 ± 9	+10 ± 22	+3 ± 8
<i>Shek Pik (SP)</i>	+62 ± 29	+11 ± 18	+70 ± 4	+28 ± 17
<i>Waglan Island (WAG)</i>	+1 ± 21	+3 ± 6	+9 ± 7	-9 ± 8
<i>Ko Lau Wan (KLW)</i>	-46 ± 39	-11 ± 17	+29 ± 65	+60 ± 57
<i>Kwai Chung (KC)</i>	-90 ± 46	-10 ± 29	-91 ± 226	-202 ± 161

762

763

764

765

766

767 **Table 3** The δ -HAT and D_1/D_2 TACs for the period of 1986-2016. The δ -HAT values given
768 are in units of millimeter change in tidal amplitude for a 1-meter fluctuation in sea level (mm
769 m⁻¹). D_1/D_2 TACs are in unitless ratios (i.e., mm mm⁻¹) Statistically significant values are
770 given in bold italic text.

<i>Station</i>	δ-HAT	D_1/D_2
<i>Quarry Bay (QB)</i>	+665 ± 82	+1.08 ± 0.05
<i>Tai Po Kau (TPK)</i>	+612 ± 210	+1.01 ± 0.04
<i>Tsim Bei Tusi (TBT)</i>	+56 ± 117	+0.37 ± 0.02
<i>Chi Ma Wan (CMW)</i>	-119 ± 19	+0.74 ± 0.19
<i>Cheung Chau (CHC)</i>	-12 ± 42	+0.81 ± 1.03
<i>Lok On Pai (LOP)</i>	-114 ± 45	+0.26 ± 0.05
<i>Ma Wan (MW)</i>	-91 ± 73	+0.57 ± 1.02
<i>Tai Miu Wan (TMW)</i>	+42 ± 100	+1.04 ± 0.20
<i>Shek Pik (SP)</i>	+138 ± 37	+0.89 ± 0.06
<i>Waglan Island (WAG)</i>	+3 ± 31	+1.11 ± 0.17
<i>Ko Lau Wan (KLW)</i>	-66 ± 47	+1.31 ± 0.62

